

AD-A095 459

ARMY ELECTRONICS RESEARCH AND DEVELOPMENT COMMAND FO--ETC F/8 17/8
PROPAGATION MODELING AND APPLICATIONS FOR ELECTRO-OPTICAL SYSTEMS--ETC(U)
OCT 80 R J BERGEMANN, L P OBERT
DELNV-TR-0016

UNCLASSIFIED

NL

1 of 1
AD-A
097459



END
DATE
FILMED
3-81
DTIC

20

12

AD

AD A095459

Report DELNV-TR-0016

LEVEL II

PROPAGATION MODELING AND APPLICATIONS
FOR ELECTRO-OPTICAL SYSTEMS

by
Richard J. Bergemann
Luanne P. Obert

DTIC
EXTRACTED
FEB 25 1981

October 1980

FILE COPY

Approved for public release; distribution unlimited.

U.S. ARMY ELECTRONICS R&D COMMAND
NIGHT VISION & ELECTRO-OPTICS LABORATORY
FT. BELVOIR, VIRGINIA 22060



81 2 24 007

Destroy this report when it is no longer needed. Do not return it to the originator.

The citation in this report of trade names of commercially available products does not constitute official endorsement or approval of the use of such products.

UNCLASSIFIED

SECURITY CLASSIFICATION OF THIS PAGE (When Data Entered)

• 318 789

| REPORT DOCUMENTATION PAGE | | READ INSTRUCTIONS BEFORE COMPLETING FORM |
|---|--|---|
| 1. REPORT NUMBER 14 DFLNV-TR-0016 | 2. GOVT ACCESSION NO. AD A095459 | 3. RECIPIENT'S CATALOG NUMBER |
| 4. TITLE (and Subtitle) PROPAGATION MODELING AND APPLICATIONS FOR ELECTRO-OPTICAL SYSTEMS | 5. TYPE OF REPORT & PERIOD COVERED Technical Report | 6. PERFORMING ORG. REPORT NUMBER |
| 7. AUTHOR(s) Richard J./Bergemann Luanne P. Obert | 8. CONTRACT OR GRANT NUMBER(s) | 9. PERFORMING ORGANIZATION NAME AND ADDRESS US Army Electronics Research & Development Command; Night Vision & Electro-Optics Laboratory; Fort Belvoir, Virginia 22060 |
| 10. CONTROLLING OFFICE NAME AND ADDRESS US Army Electronics Research & Development Command Night Vision & Electro-Optics Laboratory; Fort Belvoir, Virginia 22060 | 11. REPORT DATE Oct 1988 | 12. PROGRAM ELEMENT, PROJECT, TASK AREA & WORK UNIT NUMBERS 12 36 |
| 13. MONITORING AGENCY NAME & ADDRESS (if different from Controlling Office) | 14. SECURITY CLASS. (of this report) Unclassified | 15. NUMBER OF PAGES 38 |
| 16. DISTRIBUTION STATEMENT (of this Report) Approved for public release, distribution unlimited. | | 15. SECURITY CLASS. (of this report) Unclassified |
| 17. DISTRIBUTION STATEMENT (of the abstract entered in Block 20, if different from Report) | | 15a. DECLASSIFICATION DOWNGRADING SCHEDULE |
| 18. SUPPLEMENTARY NOTES | | |
| 19. KEY WORDS (Continue on reverse side if necessary and identify by block number) IR Propagation Fog Electro-Optical (E-O) Systems Limited Visibility Snow Realistic Battlefield Environment Natural Atmosphere Smoke Battlefield Obscurants Dust | | |
| 20. ABSTRACT (Continue on reverse side if necessary and identify by block number) Recent efforts in characterizing natural and battlefield atmospheric conditions for E-O systems performance analyses are described. Empirical aerosol scaling relationships are illustrated, along with applications to systems sensitivity studies and the determination of critical meteorological parameters. Brief descriptions of a white phosphorus (WP) smoke and a high-explosive (HE) dust model are presented. Sample predictions and comparisons to field data are shown. | | |

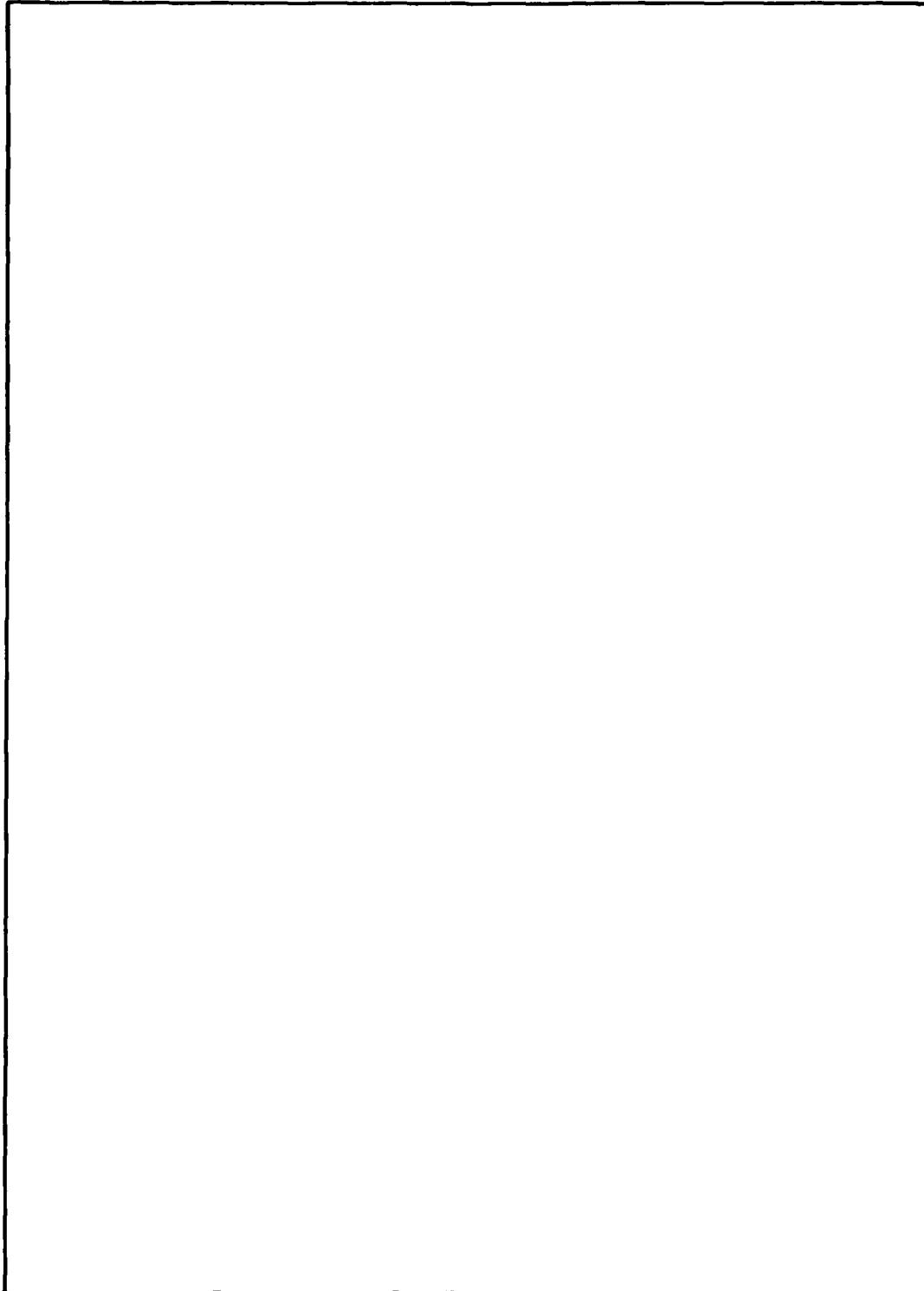
UNCLASSIFIED

SECURITY CLASSIFICATION OF THIS PAGE (When Data Entered)

318 789

UNCLASSIFIED

SECURITY CLASSIFICATION OF THIS PAGE(When Data Entered)



UNCLASSIFIED

11 SECURITY CLASSIFICATION OF THIS PAGE(When Data Entered)

ILLUSTRATIONS

| Figure | Title | Page |
|--------|--|------|
| 1 | G/AP Aerosol Model 3- to 5- μm | 3 |
| 2 | G/AP Model 8- to 12- μm | 4 |
| 3 | Snow Scattering Model 3- to 5- μm | 5 |
| 4 | Snow Scattering Model 8- to 12- μm | 6 |
| 5 | TOW Nightsight Capability | 8 |
| 6 | Meteorological Conditions Required for Different Capability Levels | 9 |
| 7 | Elements of NV&EOL/GRC Smoke Model | 11 |
| 8 | Comparison of Plume Model to JPG Data | 12 |
| 9 | Comparison of NV&EOL/GRC Model to WSMR Test Data | 14 |
| 10 | Comparison of NV&EOL/GRC Model to DPG Data | 15 |
| 11 | Comparison of NV&EOL/GRC Model to DPG Data | 15 |
| 12 | Comparison of NV&EOL/GRC Model to DPG Data | 15 |
| 13 | Comparison of NV&EOL/GRC Model to DPG Data | 15 |
| 14 | Configuration of Smoke Barrage | 16 |
| 15 | Barrage Transmission History | 17 |
| 16 | Elements of HE Dust Model | 20 |
| 17 | Predicted vs. Measured Cloud Height | 21 |
| 18 | Predicted vs. Measured Transmission (8- to 12- μm) | 21 |

ILLUSTRATIONS (CONT'D)

| Figure | Title | Page |
|--------|--|------|
| 19 | Predicted vs. Measured Cloud Height | 22 |
| 20 | Predicted vs. Measured Transmission (8- to 12- μm) | 23 |
| 21 | Comparison of HE Dust Model to Ft. Sill Data | 24 |
| 22 | Comparison of HE Dust Model to Smoke Week II Data | 25 |

TABLES

| Table | Title | Page |
|-------|---|------|
| 1 | Recognition (NFOV) | 10 |
| 2 | Time (s) 8- to 12- μ m Transmission \leq 1% | 18 |

PROPAGATION MODELING AND APPLICATIONS FOR ELECTRO-OPTICAL SYSTEMS

I. INTRODUCTION

The need to evaluate the performance of electro-optical (E-O) systems in the natural and battlefield environment has, in recent years, generated a flurry of activity directed at the measurement and modeling of the atmosphere. As the emerging results of these efforts are applied to the analysis of E-O systems, a new understanding of the utility and limitations of such devices is now developing. Some of these measurement, modeling, and analysis activities are reported here.

In Section II, the fog and snow multispectral transmission data base that has been collected over the last 4 years is described. Simple algorithms representing this data are derived. Section III outlines a study of TOW system performance sensitivity to changes in the meteorology of the environment. Considerations of target signature variability are taken into account. Results from such a study can be used to establish critical meteorological parameters associated with system performance. A discussion of this can be found in Section IV.

Sections V and VI present a brief description, sample predictions, and validation of two models for battlefield obscuration. Section V addresses a model for instantaneous white phosphorus (WP) smoke, and Section VI addresses a model for high-explosive (HE) dust. Both models are a subset of the total obscuration modeling performed by NV&EOL and the General Research Corporation (GRC).^{1 2 3}

II. AEROSOL TRANSMISSION THROUGH THE NATURAL ATMOSPHERE

Absolute atmospheric transmission measurements in the visible, near IR, 3- to 5- μm and 8- to 12- μm regions have been collected through various fogs that have been observed at Ft. A. P. Hill, Virginia; Grafenwoehr, Germany; and Baumholder, Germany. Portions of this data have been previously reported,⁴ but Figures 1 and 2 show the present data base

¹ The semi-empirical models were formulated by Dr. R. Zirkind, General Research Corp., under Contract No. DAAK02-74-C-0366 with the U.S. Army Night Vision and Electro-Optics Laboratory, Ft. Belvoir, VA. Mrs. L. P. Obert, contract monitor. The contractual effort provided models which are more comprehensive than focused upon here. (The reader is referred to documentation in References 2 and 3).

² R. Zirkind, "An Obscuring Aerosol Dispersion Model," Vols. I & II, CR-231 for US Army NV&EOL under Contract No. DAAK02-74-C-0366 by General Research Corp., McLean, VA, Dec 78 (Unclassified).

³ R. Zirkind, "A Preliminary Description of an Explosive Dust Cloud Model," Tech Memorandum for US Army NV&EOL under Contract No. DAAK02-74-C-0366 by General Research Corp., McLean, VA, Dec 78 (Unclassified).

⁴ J. R. Moulton, R. J. Bergemann, and M. C. Sola, "U. European Winter Atmospheric Environment (U)," IRIS Proceedings, Aug 76 (Secret).

in its entirety. As a general rule, systematic scaling between visible, 3- to 5- μm , and 8- to 12- μm aerosol extinction has been found, with the cleanest relationships associated with data collected in individual fogs.

Figure 1 shows curve fits to the data relating visible and 3- to 5- μm extinction through fog. The wet and dry curves are fits to data subsets defined by observed meteorological conditions. The "wet" condition is indicative of a high-aerosol moisture content. Each day of data was classified as wet or dry by its predominant optical character when an on-site determination of the fog's nature was not made. The middle curve, as noted, is a fit to all of the data. The relationship between visible extinction and that in the 8- to 12- μm bandpass is shown in Figure 2.

The equations corresponding to the curve fits shown in Figures 1 and 2 are the following:

$$\begin{aligned}
 \text{WET FOG: } \quad \sigma_{3-5} &= 10^{-.917 + 2.595 \log \sigma_{vis} -.782 (\log \sigma_{vis})^2} \\
 \sigma_{8-12} &= 10^{1.144 + 2.871 \log \sigma_{vis} -.895 (\log \sigma_{vis})^2} \\
 \text{DRY FOG: } \quad \sigma_{3-5} &= 10^{1.667 + 3.398 \log \sigma_{vis} -.863 (\log \sigma_{vis})^2} \\
 \sigma_{8-12} &= 10^{1.712 + 2.565 \log \sigma_{vis} -.328 (\log \sigma_{vis})^2} \\
 \text{COMBINED: } \quad \sigma_{3-5} &= 10^{1.0 + 2.404 \log \sigma_{vis} -.511 (\log \sigma_{vis})^2} \\
 \sigma_{8-12} &= 10^{.98 + 1.851 \log \sigma_{vis} -.212 (\log \sigma_{vis})^2} \\
 \sigma_{.55} &= 10^{.239 + .751 \log \sigma_{vis} -.281 (\log \sigma_{vis})^2}
 \end{aligned}$$

Additional data gathered at 1.06 μm has resulted in the scaling law that is also shown above. These formulations are currently being used to evaluate E-O systems performance under limited-visibility conditions.

Data has also been gathered under conditions of snow. Figures 3 and 4 show visible vs. 3.9- μm data and visible vs. 8- to 12- μm data collected at Ft. A. P. Hill, Virginia, and previously reported.⁵ The resultant extinction relationships due to snow alone have been derived, correcting the original data for molecular absorption and fog/haze attenuation. The correction factors were determined during snowfall-free periods contiguous to actual measurement times. *Note that some severe fog that occurred during the measurements had a dramatic effect on the extinction relationships.* More generally, it is apparent that the mixed haze/fog/snow condition is important since this is the way snow appears in nature.

⁵ M. Sola and R. Bergemann, "Multi-spectral Propagation Measurements Through Snow," Tech. Digest of the Top. Meeting on Opt. Prop. through Turb., Rain & Fog, OSA, Aug 77 (Unclassified).

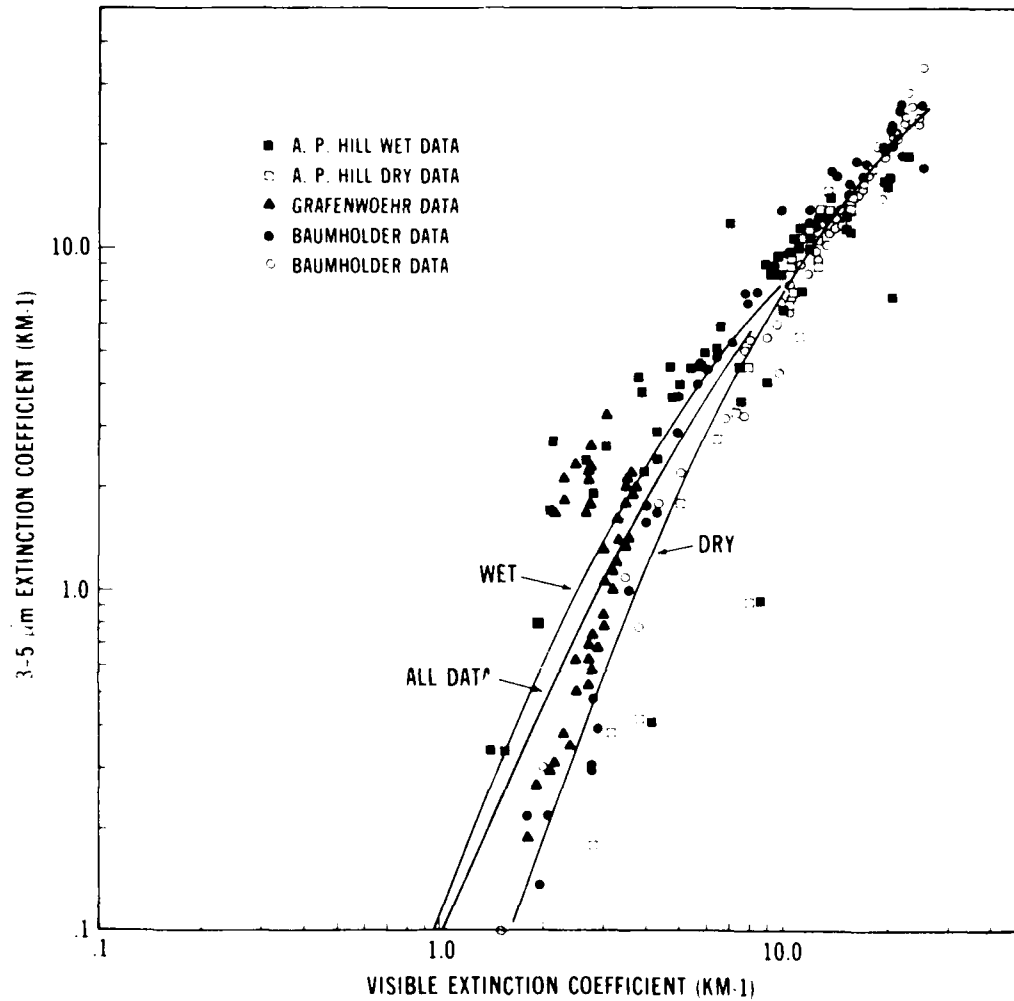
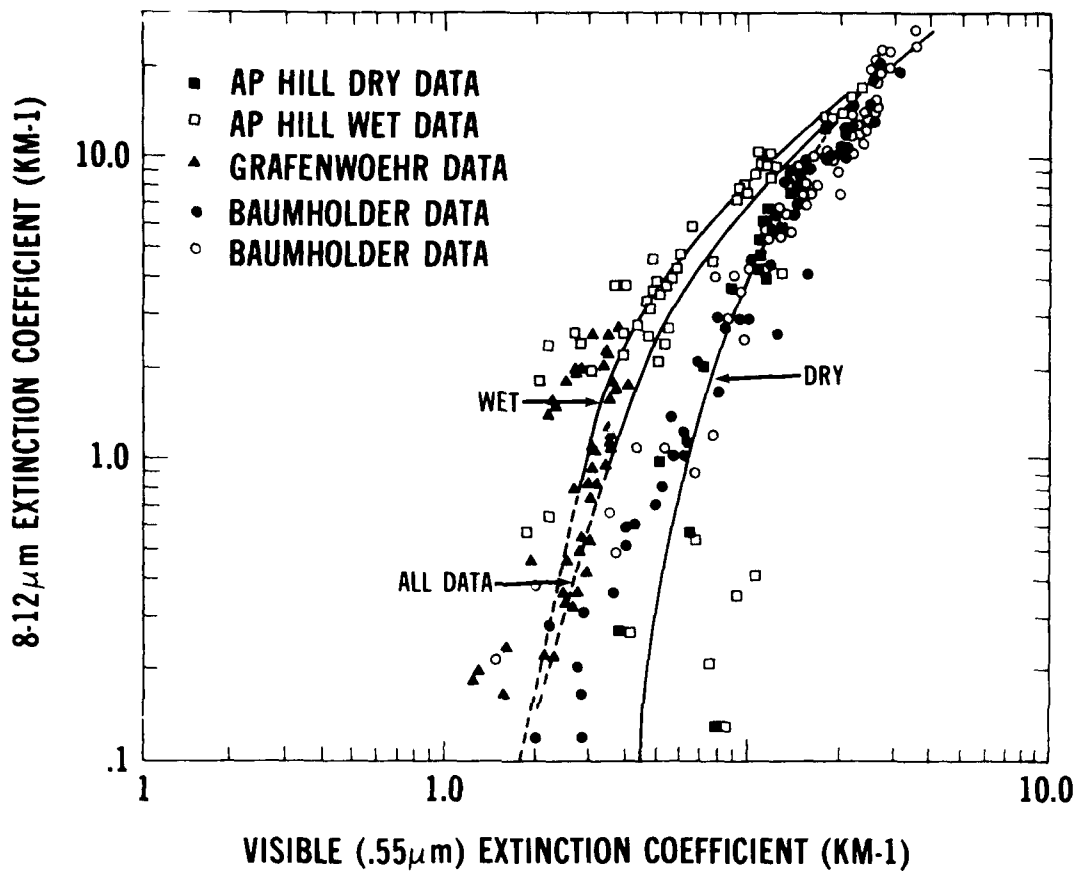


Figure 1. G/AP aerosol model 3- to 5- μm .
 (Low visibility aerosol attenuation data and
 derived empirical fits for locations in Virginia and Germany.)



VISIBLE (.55 μm) EXTINCTION COEFFICIENT (KM-1)

Figure 2. G/AP model 8- to 12- μm .
 (Low visibility aerosol attenuation data and
 derived empirical fits for locations in Virginia and Germany.)

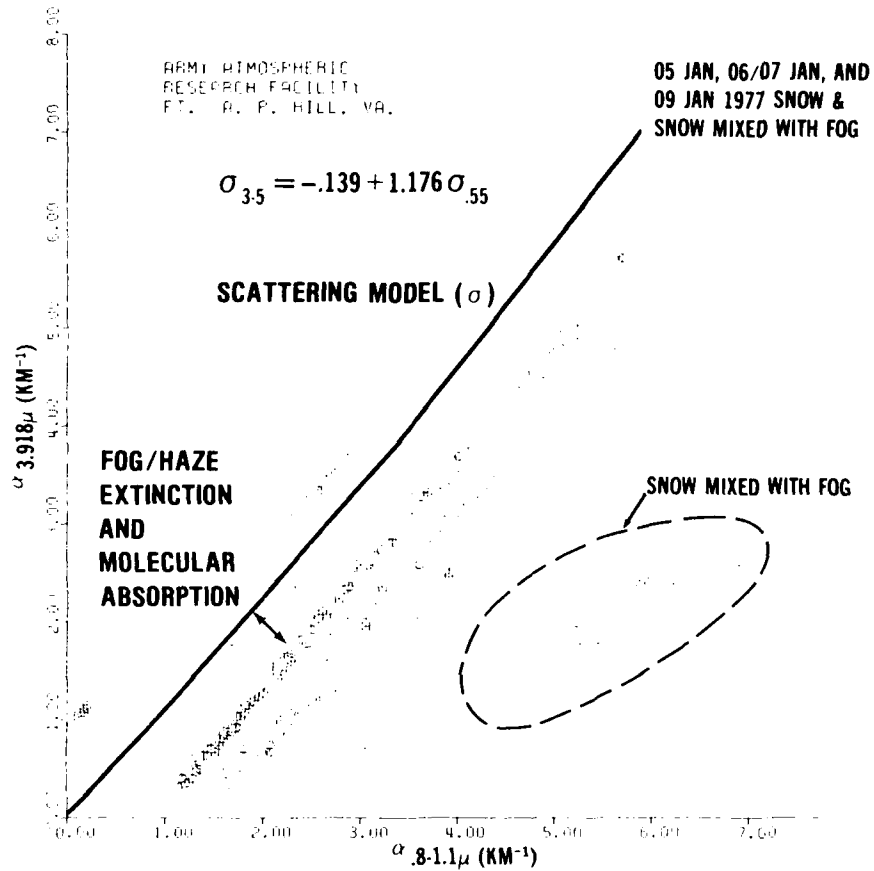


Figure 3. Snow scattering model 3- to 5- μ m.
(Extinction data taken through snow at A. P. Hill, Virginia,
showing the relationship between the visible-near IR and 3.918 μ m.)

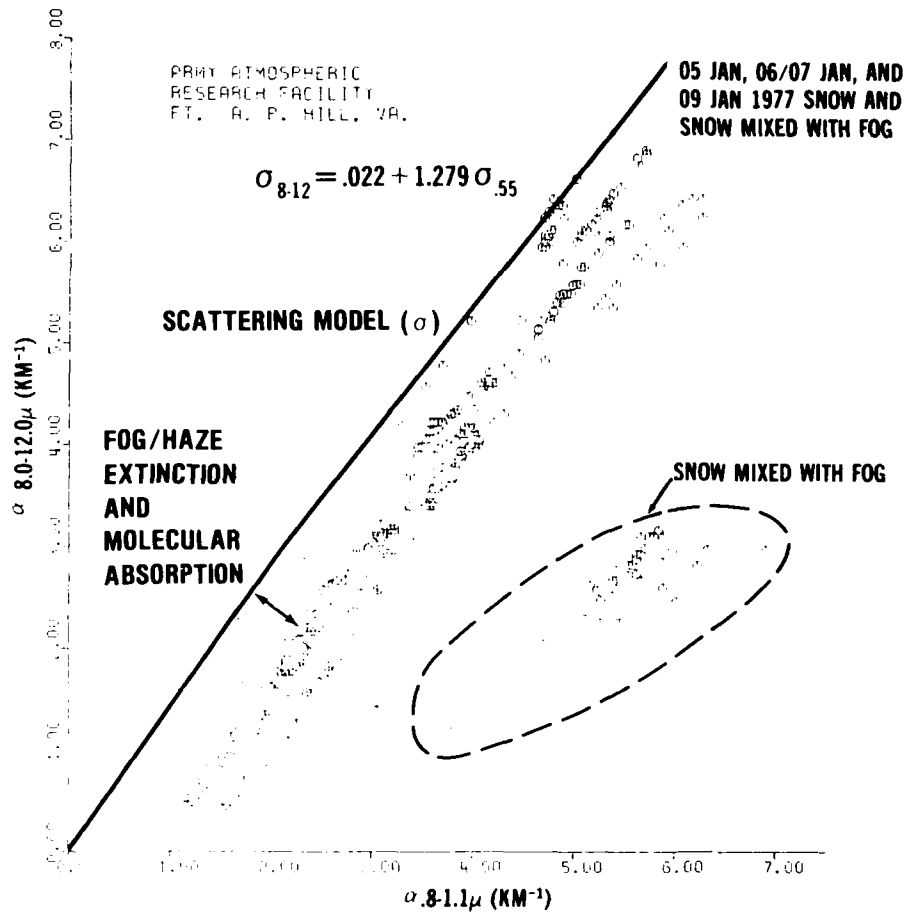


Figure 4. Snow scattering model 8- to 12- μ m.
(Extinction data taken through snow at A. P. Hill, Virginia, showing
the relationship between the visible-near IR and 8.0 to 12.0 μ m.)

III. TOW SYSTEM PERFORMANCE SENSITIVITY

Using the G/AP aerosol model described in Section II, an investigation of the sensitivity of the TOW nightsight performance to changes in the air temperature, relative humidity, visibility, and target signature was conducted. Results were represented in terms of R/R_0 , where R_0 is the maximum performance range (50% probability) for a given season and target condition assuming no atmospheric limitations. Three signature strengths were chosen to represent the spread in measured signatures of a tank viewed from the front or the side in summer or winter. Appropriate seasonal background temperatures were used. Signature data was obtained from the Night Vision and Electro-Optics Signature Data Base.

For real atmospheric conditions, the variation in R/R_0 as a function of visibility and relative humidity is shown in Figure 5. For this summer condition, it is apparent that at low visibilities the aerosol effect dominates and there is virtually no variation in performance with atmospheric water content. At the longer visibility ranges, it is absorption that dominates.

If a certain value of R/R_0 can be established as necessary to accomplish a particular military task, henceforth referred to as a level of capability, Figure 5 can be presented in a manner that shows what combinations of meteorological conditions will allow at least that capability level. As an example, Figure 6 defines those meteorological conditions that result in a 50% and an 80% capability level over the summer (S) and winter (W). The most significant thing to note is that certain system capability levels are insensitive to large-scale variations in the atmospheric water content. In general, however, higher levels of system capability show the more complex dependence on water vapor.

IV. CRITICAL METEOROLOGICAL PARAMETERS

The study described in Section III indicates that, for certain levels of system capability, a critical meteorological parameter can be defined. In the case of the TOW nightsight at a 50% level of capability, this meteorological parameter is visibility. The visibility range required is relatively constant over a wide range of variation in target ΔT , target aspect, and season. The results shown in Table 1 indicate that a visibility of greater than about a kilometer defines that condition when the TOW nightsight will perform to at least 50% of its theoretical capability. Results for the WFOV detection task are essentially the same.

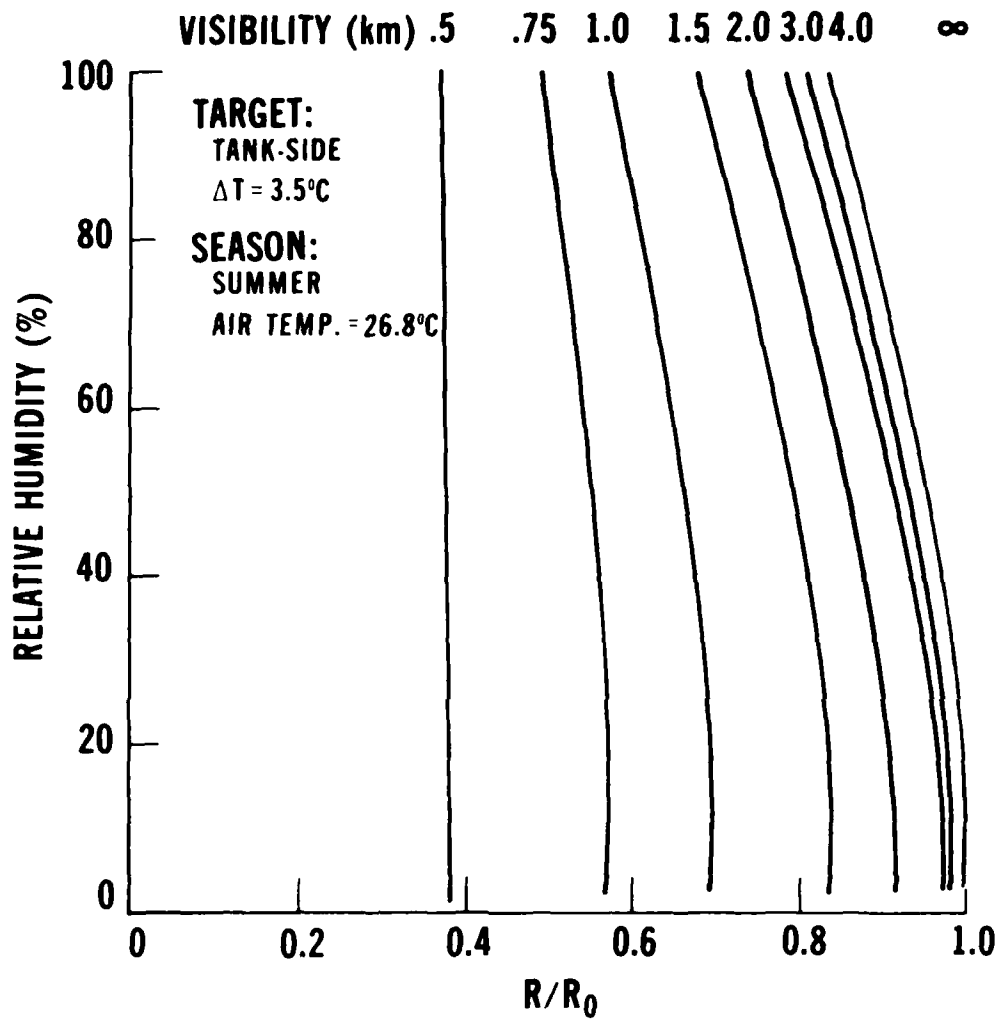


Figure 5. TOW nightsight capability.
 (For a 50% recognition probability of the side view of a summer tank.)

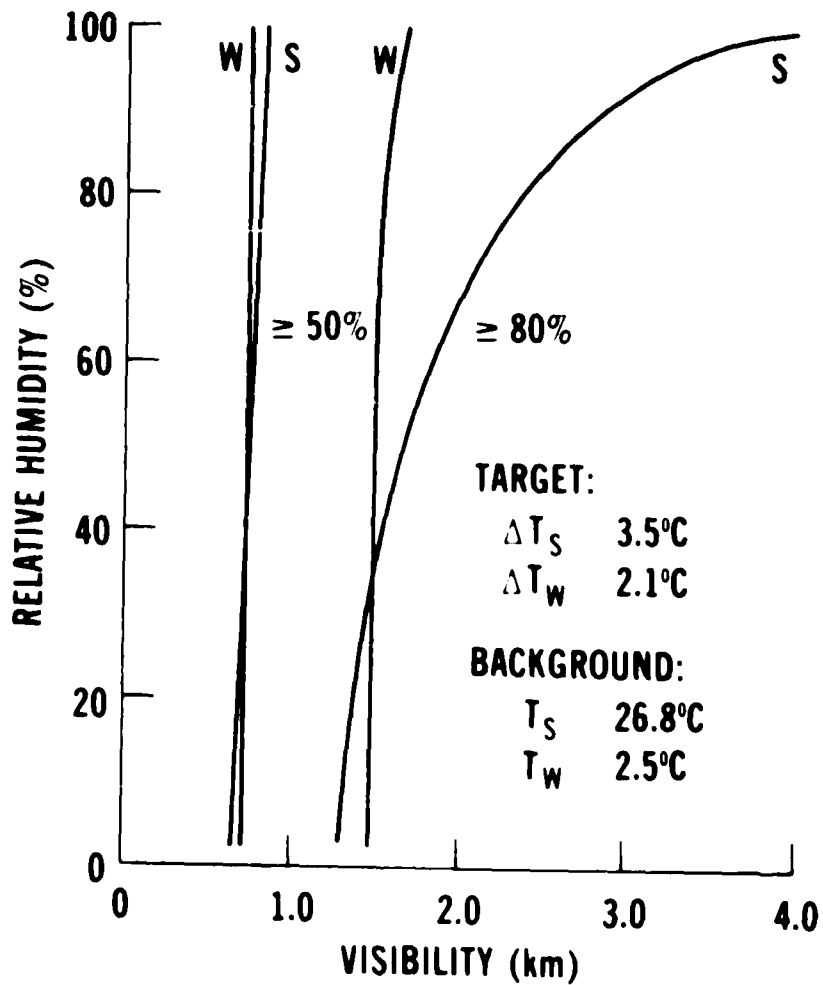


Figure 6. Meteorological conditions required for different capability levels. (At a 50% recognition probability of a summer (S) or winter (W) tank-side view.)

Table 1. Recognition (NFOV)

| Target | Season | Target R1 | | |
|------------|--------|-----------|---------|---------|
| | | High | Medium | Low |
| Tank Side | Summer | 8.7 km | 6.8 km | 7.9 km |
| | Winter | 6 km | 7 km | 7 km |
| Tank Front | Summer | 6.9 km | 7.10 km | 8.11 km |
| | Winter | 8 km | 9 km | 9 km |

V. NV&EO/GR WP SMOKE MODEL

The goal of the design of both the WP smoke model and the HE dust model which is described in Section VI was to develop simple semi-empirical formulations which would be compatible with the target-acquisition processes for EO sensor performance in combat simulations. Transmission and spatial characterization of the three-dimensional cloud, both as a function of time, were considered prime ingredients of the modern battlefield for predicting the performance of EO systems operating in the visible through Far IR spectral regions. The models were designed to utilize readily available inputs which describe the tactical scenario, barrage, meteorological conditions, and soil structure. However, it is left to the user to supply routines to tactically deploy the smoke and dust.

The WP smoke model is for point source, instantaneous WP smoke. The model exists in a stand-alone, computerized form and is modular as outlined in Figure 7. Validation results of the model to the present data set have previously been reported.² Samples of the validation results for cloud height, Concentration x Length (CL), and transmission are presented in the following paragraphs. Finally, the prediction possibilities are illustrated by applying the WP smoke model to a barrage scenario.

1. Cloud Height Comparison. The first example of validation in Figure 8 compares the prediction for cloud height to data measured at Jefferson Proving Ground by the US Army Materiel Systems Analysis Activity. The measured cloud-height data as a function of time is indicated by the dots for a 105-mm, statically fired WP smoke round. Predictions by the model are represented by the dashed curves for the range of measured wind speeds of 1 to 2 meters/second with the atmospheric stability characterized as slightly unstable.

² "The NV&EO/GR WP Smoke Model," *Proceedings of the 1987 Army Materiel Systems Analysis Activity Conference*, 1987, pp. 1-10.

³ "The NV&EO/GR HE Dust Model," *Proceedings of the 1987 Army Materiel Systems Analysis Activity Conference*, 1987, pp. 1-10.

CANDIDATE SMOKE MODEL

ARTILLERY DELIVERED, SINGLE MUNITION

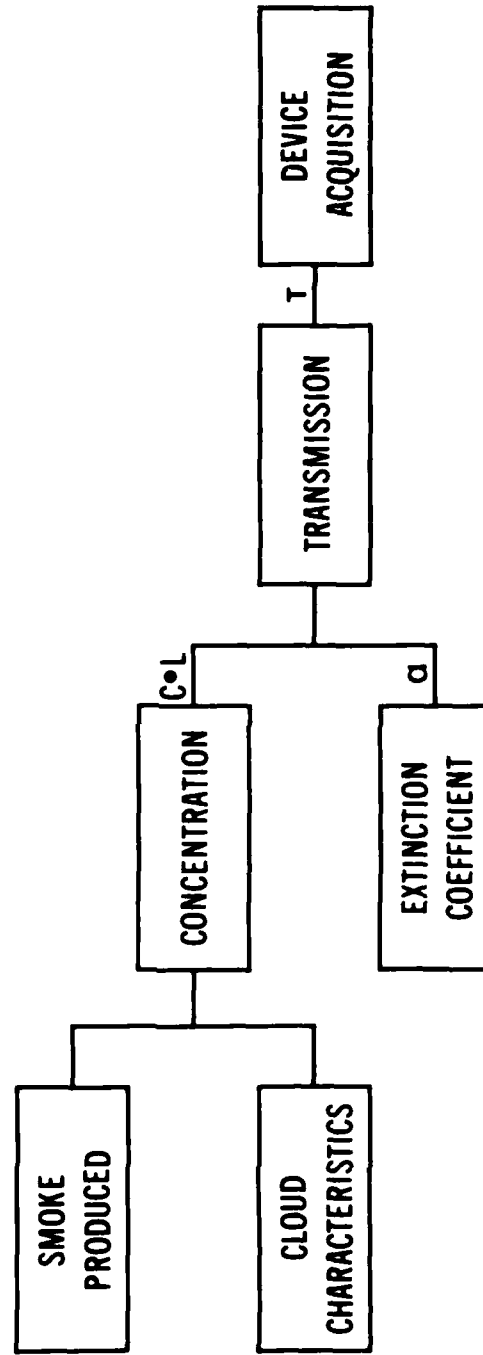
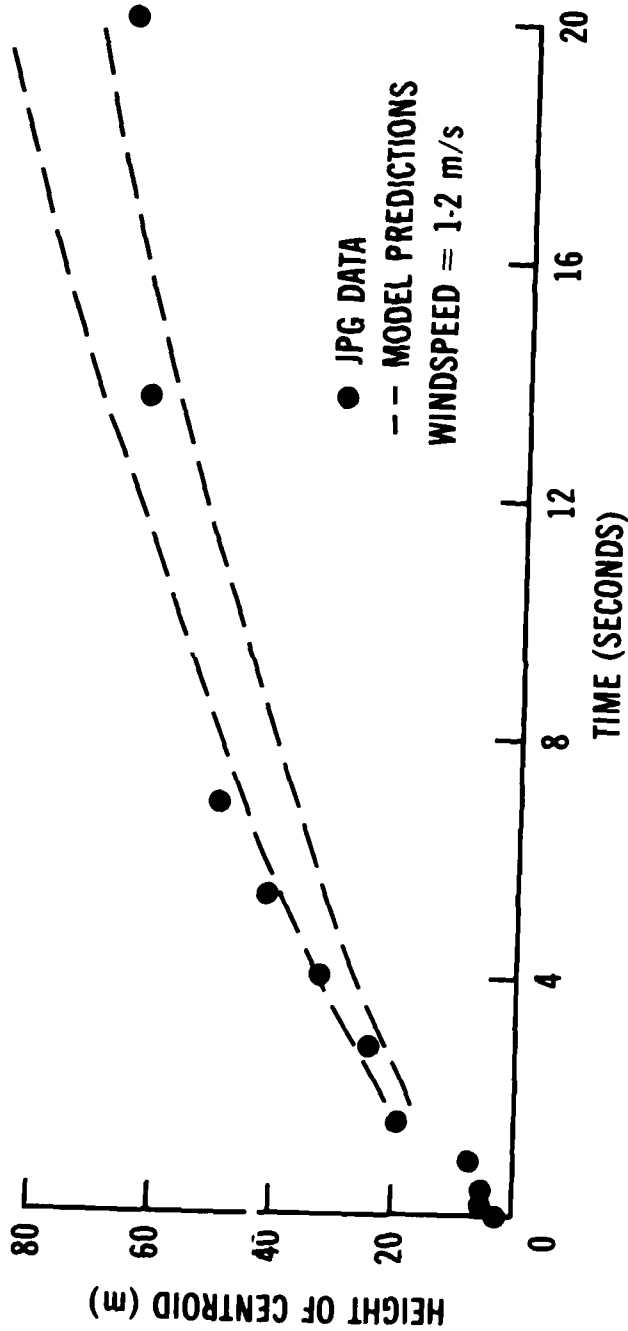


Figure 7. Elements of NV&EOL/GRC smoke model. (Instantaneous WP.)



PLUME RISE, 105mm WP, STATIC FIRING, PASQUILL CATEGORY C

Figure 8. Comparison of Plume model to JPG data. (Static firing, 105-mm WP, Pasquill category C.) (Reference 7)

2. CL Comparison. Figure 9 shows the comparison of model predictions to CL measurements. The data is from the smoke trials at White Sands Missile Range (WSMR) conducted by the PM Smoke/Obscurants in July 77.⁶ Trail 9 (WP-3) consisted of the static firing of five 4.2-in. WP rounds. Sharp rises and falls of the measured data may be attributed to variation in windspeed and direction. Predictions which are based on inputs of the average meteorological parameters reported in Figure 9 plus the geometry of the test configuration are indicated by the dashed curve.

3. Transmission Comparison. The final sample of validation in Figures 10 through 13 compares predictions to measured transmission from Smoke Week 1 at Dugway Proving Ground conducted by the PM Smoke/Obscurants in November 77.⁷ Transmission versus time was measured by transmissometers in the Far IR, Mid IR, 1.06- μm and visible spectrum bands over the same sampling line. Illustration of the agreement between predicted and measured data for trial 34 which consisted of six 155-mm, statically fired, WP smoke rounds is shown for transmission in the 8- to 12- μm (Figure 10), 3.4- μm (Figure 11), 1.06- μm (Figure 12), and visible (Figure 13) regions.

4. Smoke Barrage Predictions. The illustration of capabilities of the WP smoke model is concluded with a prediction of transmission for a smoke barrage. The layout of the barrage scenario as depicted in Figure 14 consists of two volleys of 155-mm WP smoke. The X's indicate the impact points of the first volley of 15 rounds which are uniformly distributed over the 1 kilometer front at time zero. The O's represent the impact points of the second volley of 15 rounds which are uniformly distributed over the front and spaced between the initial rounds at time zero plus 30 seconds.

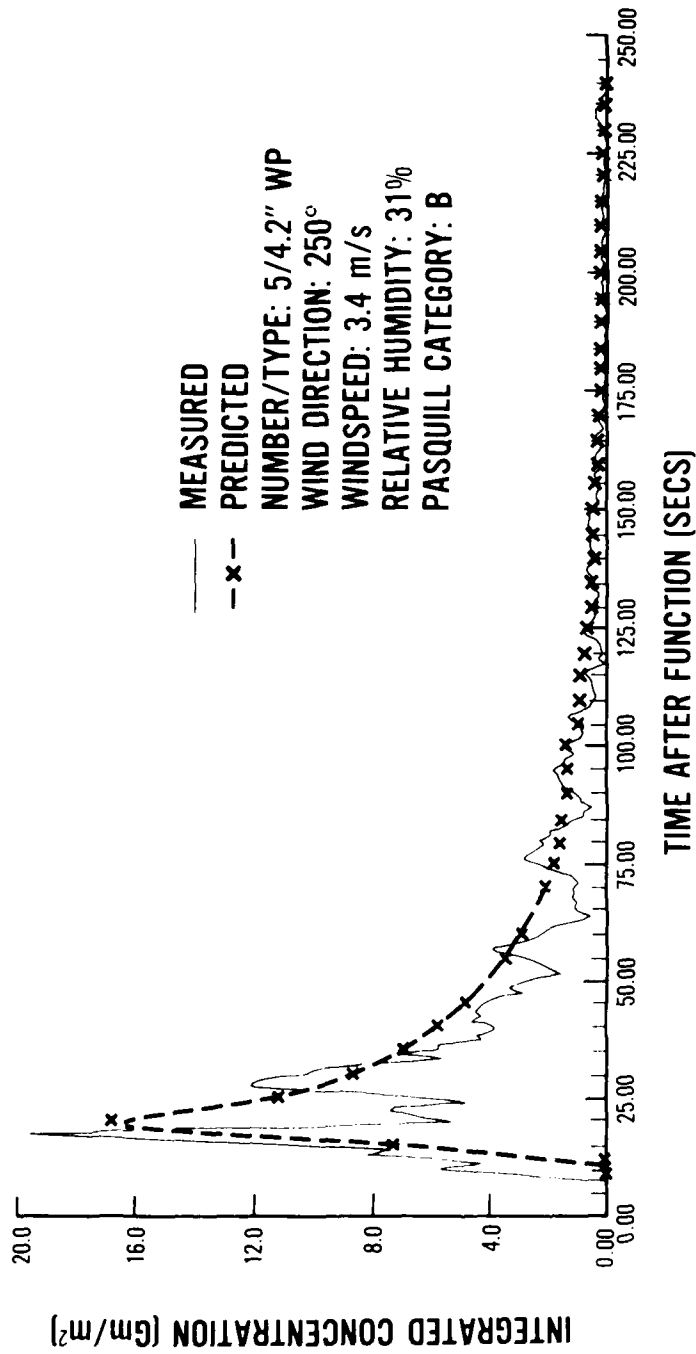
The growth as a function of time of several of the clouds of the initial volley is illustrated. The length of each cloud is indicated along a time axis with 10-second tick marks out to 2 minutes. The other dimension illustrated is the width of the cloud. The purpose of the cloud depiction is to illustrate the intersection of the clouds with the observer-target line-of-sight (LOS) as a function of time. At 2 minutes, four rounds of the initial volley and three rounds of the second volley intersect the LOS.

Transmission for 8- to 12- μm versus time after initiation of the barrage is plotted in Figure 15 for three atmospheric stability conditions: moderately unstable, neutral, and moderately stable, i.e., Pasquill Categories B, D, and E, respectively. The first-minute effects are highly dependent on the geometry, i.e., intersection of the clouds with the LOS. In order to relate these predictions with the GRAF II trials,⁸ the

⁶ Manportable Common Thermal Night Sight Smoke Test at White Sands Missile Range July 77 (C) PM-SMK-1000-20 (Uncl. DIR No. ADO-C1-243) (Confidential)

⁷ Smoke Week 1: Electro-Optical (EO) System Performance in Characterized Smoke Environment at Dugway Proving Ground (C) No. 1000-20 (Uncl. DIR PM-SMK-1000-20, Apr 78, DIR No. ADO-C1-528) (Confidential)

⁸ J.R. McArthur and J.W. Casady, "Correlations for IR Radiative Battlefield Sensor Levels," Winter 47, Proceedings of the 25th National IRIS Meeting, 1978.



TRIAL 9 (WP-3), JULY 20 1977, 23:12:52, WP SMOKE
CONCENTRATION INTEGRATED ACROSS SIGHT LINE

Figure 9. Comparison of NV&EOL/GRC model to WSMR test data.
(Trial 9 (WP-3), 20 Jul 77, WP smoke concentration integrated across sight line.) (Reference 8)

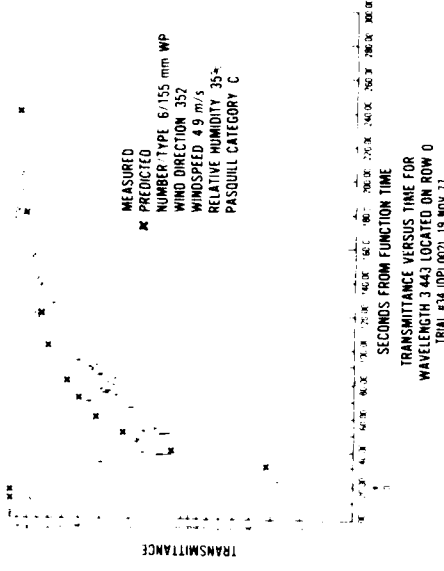


Figure 10. Comparison of NV&EOL/GRC model to DPG data. (Transmission versus time for wavelength 9.750 μm located on row 0; Trial #34 (DPI-002), 19 Nov 77.) (Reference 9)

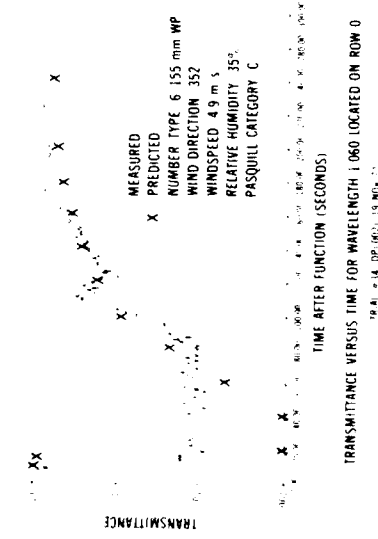


Figure 11. Comparison of NV&EOL/GRC model to DPG data. (Transmission versus time for wavelength 3.443 μm located on row 0; Trial #34 (DPI-002), 19 Nov 77.) (Reference 9)

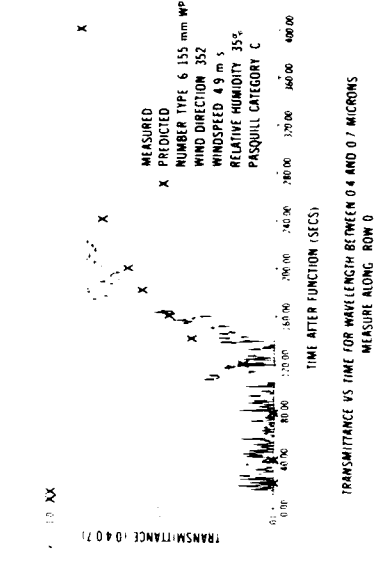


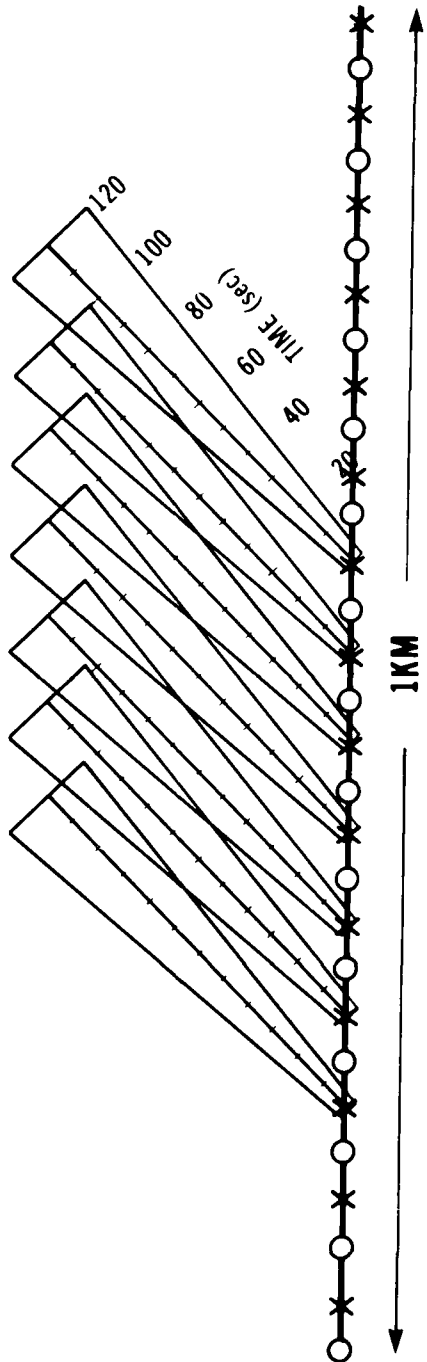
Figure 12. Comparison of NV&EOL/GRC model to DPG data. (Transmission versus time for wavelength 1.06 μm located on row 0; Trial #34 (DPI-002), 19 Nov 77.) (Reference 9)

Figure 13. Comparison of NV&EOL/GRC model to DPG data. (Transmission versus time for wavelength between 0.4 and 0.7 μm measured along row 0; Trial #34 (DPI-002), 19 Nov 77.) (Reference 9)

TYPE : 155mm WP
 WIND DIRECTION : 45°
 WIND SPEED : 5 Kts
 RELATIVE HUMIDITY : 80%
 PASQUILL CATEGORY : D

X - 1st VOLLEY - 15 Rds/Km AT t_0
 O - 2nd VOLLEY - 15 Rds/Km AT $t_0 + 30$ sec

TARGET ↑



↓
OBSERVER

Figure 14. Configuration of smoke barrage.

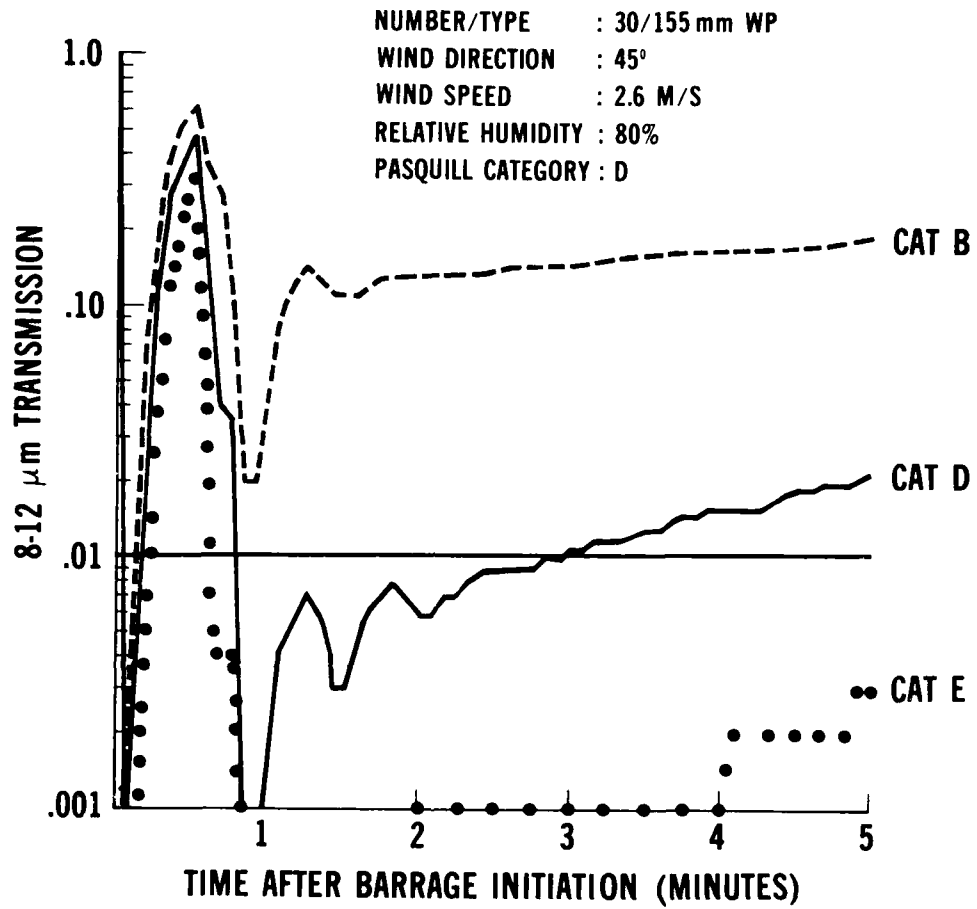


Figure 15. Barrage transmission history.

1% transmission level is chosen as a threshold of interest. Table 2 is a summary of the time that the 8- to 12- μm transmission is below 1% (excluding the first minute of the barrage). Predictions are being prepared for the Graf II summer trials in which nonuniformity of impacts is considered.

Table 2. Time (s) 8- to 12- μm Transmission $\leq 1\%$

| Relative Humidity (%) | Pasquill Category | | |
|-----------------------|-------------------|-----|------------|
| | B | D | F |
| 40 | 0 | 0 | 150 |
| 80 | 0 | 115 | ≥ 240 |

VI. THE DUST MODELING EFFORTS

NV&EOL conducted the Graf II Realistic Battlefield Sensors Trials from 6-22 November 1978 at Grafenwoehr, Germany. The purposes of these experiments were: (1) to determine the effects of artillery barrage obscurants on E-O sensor performance, and (2) to quantify the optical propagation and transport properties of artillery-induced dust clouds.

Prior to the test, NV&EOL requested from GRC and Aerodyne Research, Inc.¹¹ predictions for the description of the dust cloud formed from single and multiple 155-mm HE rounds, artillery delivered, point detonation. Both contractors worked with NV&EOL in the planning phases of Graf II to identify any parameter gaps required by their models. Predictions of the following properties of the dust cloud were supplied to NV&EOL prior to the test: (1) dust cloud dimensions vs. time (GRC and Aerodyne); (2) Concentration x Length vs. time (GRC); (3) estimation of the mass extinction coefficients, visible through Far IR (GRC and Aerodyne); (4) transmission vs. time (GRC and Aerodyne); and (5) thermal history vs. time (GRC).

Both GRC, under continuing contractual effort with NV&EOL, and Aerodyne, under contract with Atmospheric Sciences Laboratory (ASL),¹² have been working with the Graf II results in order to expand their model development. Aerodyne's efforts are described by Ebersole, et al.¹³ Comparisons of predictions of the GRC HE Dust Model to Graf II results and other recent field tests are presented herein.

¹¹ "Description of Dust Cloud Observation for Graf II," Aerodyne Research, Inc., U.S. Army Night Vision & Electro-Optics Laboratory, Contract No. DAAG 09-78-M-1763, Sep. 78 (unclassified).

¹² Atmospheric Sciences Laboratory effort with Aerodyne Research, Inc., Battle Laboratories, Contract No. 00N 79-100.

¹³ E. Ebersole, R. V. J. Lee, M. Carnie, E. Ober, and E. Duncan, "An Analysis of Recent Infrared Observation Army Artillery Data," 1978, U.S. Army Proceedings of 27th Annual IRIS, May 79 (Secret).

In addition to predictions, GRC supplied NV&EOL with a first-cut HE dust model prior to the Graf II test. The formulation of the model is outlined in Figure 16. Outputs consist of temperature, dimensions, Concentration x Length, and transmission of the cloud.

Predictions of the model are presently being compared to field test results and are described in the following paragraphs.

1. Graf II, Event A Comparison. Event A consisted of a single 155-mm, artillery-fired HE round which intersected the transmission line-of-sight upon impact. Meteorological conditions were defined as windspeed = 3.4 m/s, wind direction = 270°, and Pasquill Category = C.

Silicon and thermal cloud height measurements and predictions for the visible height are shown in Figure 17. Predictions were calculated from the initial model in which cloud rise was not a function of cloud heat and the modified model with a heat-rise term.

The first-cut dust model assumed that thermal effects within the dust cloud were negligible. The cloud of a 155-mm HE round was predicted to reach equilibrium at 0.75 second. For time greater than 0.75 second, the cloud was dispersed as a function of wind momentum and atmospheric stability. As evidenced in the conclusions of the Graf II test results, heat was apparent in the cloud for approximately 10 seconds. Thus, an additional cloud-rise term due to the exothermic reaction has been added to the initial model. The thermal buoyancy term is identical to that of the NV&EOL/GRC WP Smoke Model with a heat release of 300 cal/g. After 10 seconds, the cloud rise is assumed to be due purely to momentum. Predictions for the 8- to 12- μ m transmission of the main cloud and stem are compared to measured transmission in Figure 18. The stem of the cloud at equilibrium was predicted to be 2.7 meters high for 155-mm HE. Although predictions of CL and transmission for both the cloud and stem were separate model calculations, the emphasis of original predictions was on the cloud. However, it has been determined that the transmission line-of-sight intersected the dust clouds at 2 to 3 meters. The predictions are now for the upper part of the stem/lower cloud area.

2. Graf II, Event B Comparison. Event B consisted of two HE rounds impacting simultaneously. Round 1 intersected the transmission line-of-sight while Round 2 was 25 meters off the line-of-sight. Meteorological conditions were defined as: windspeed = 2.5 m/s, wind direction = 270°, and Pasquill Category = C.

Measurements of cloud height of Round 1 and predictions using the heat-rise term are compared in Figure 19.

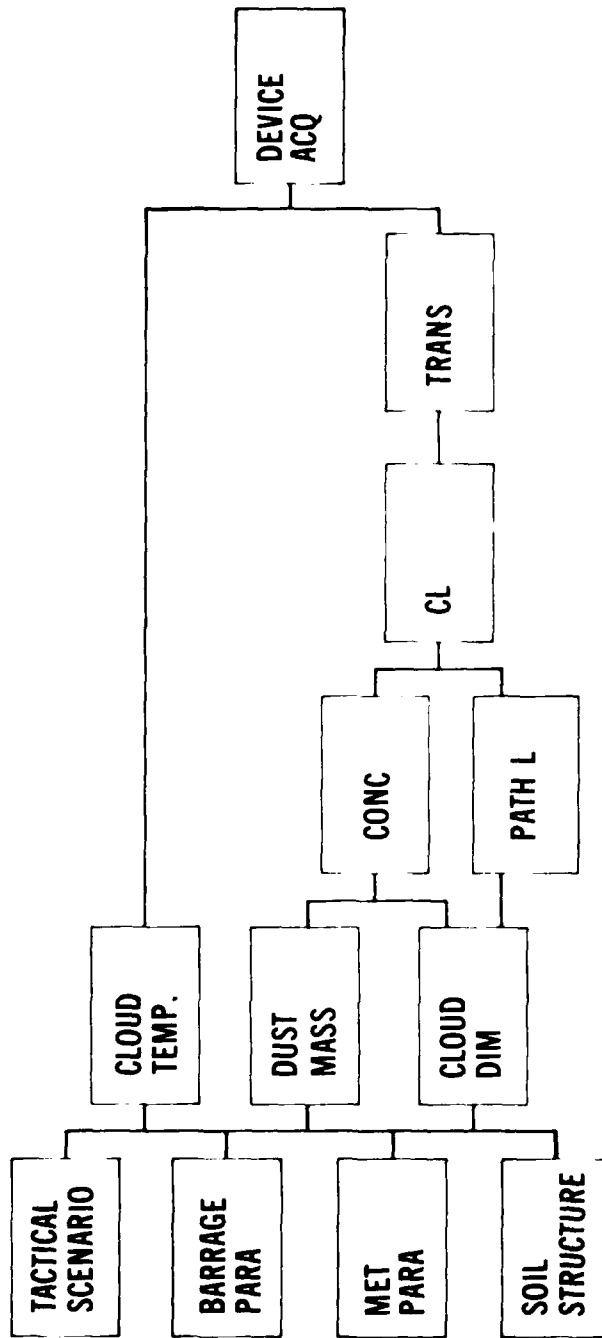


Figure 16. Elements of HE dust model.

**PREDICTED VS. MEASURED CLOUD HEIGHT
EVENT A**

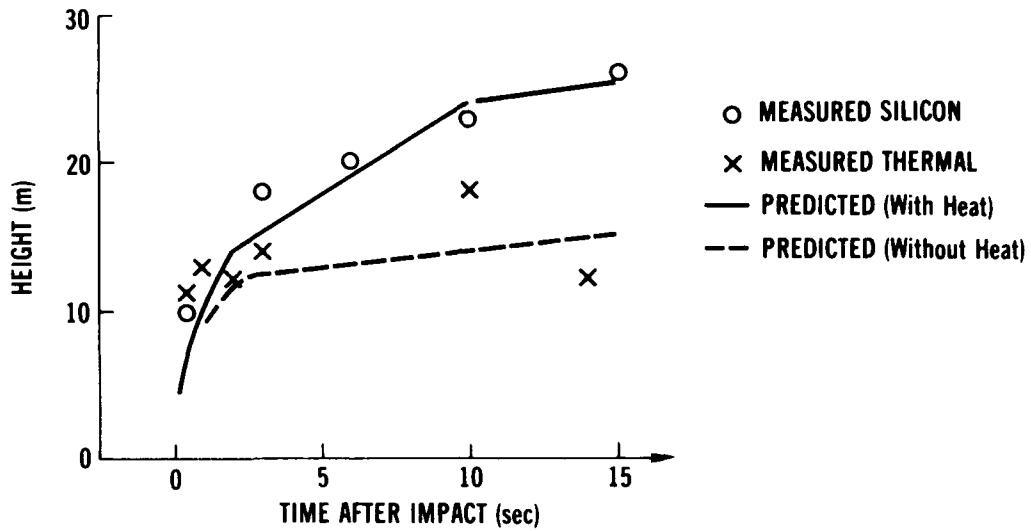


Figure 17. Predicted vs. measured cloud height. (Graf II, 10 Nov 78) (Reference 10)

**PREDICTED VS. MEASURED TRANSMISSION (8-12 μm)
EVENT A**

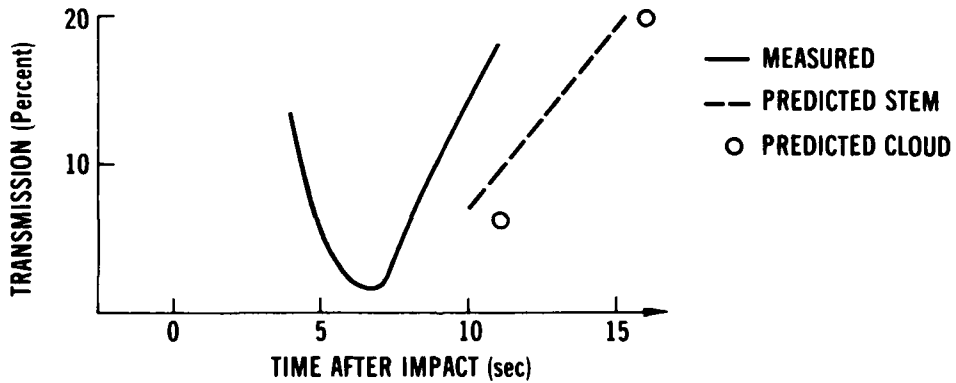


Figure 18. Predicted vs. measured transmission (8- to 12- μm). (Graf II, 10 Nov 78.) (Reference 10)

**PREDICTED VS. MEASURED CLOUD HEIGHT
EVENT B**

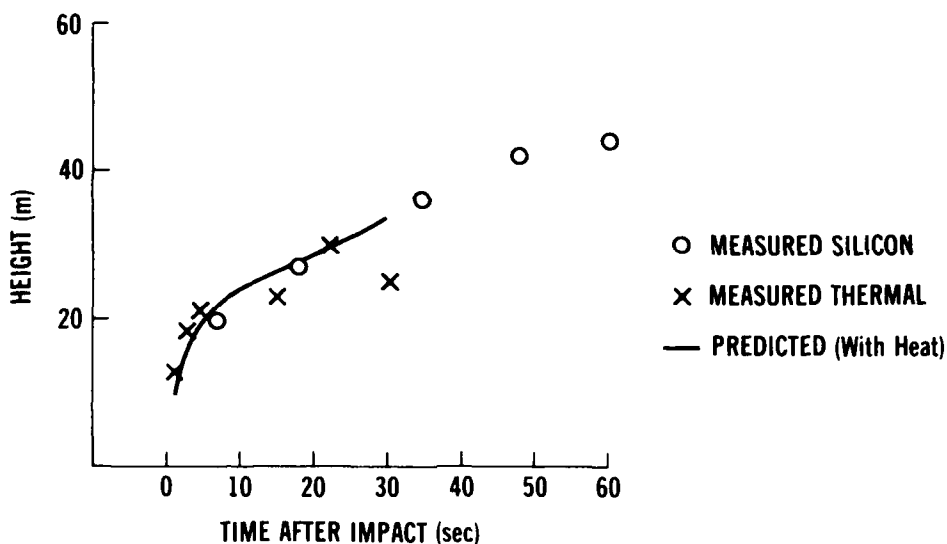


Figure 19. Predicted vs. measured cloud height. (Graf II, 17 Nov 78.) (Reference 10).

Measured and predicted 8- to 12- μm transmissions are compared in Figure 20. The effects of Round 2 are reflected in the transmission at 20 seconds from impact.

3. Ft. Sill Comparison. Artillery HE firings were conducted, and the resulting dust was characterized at Ft. Sill, Oklahoma, in May 78 for PM Smoke/Obscurants.¹⁴

Measured and predicted CLs for trial DPI-005-T3, one round of 155-mm HE, are compared in Figure 21.

4. Smoke Week II Comparison. Measured and predicted CLs are placed in Figure 22 for trial No. 29, six rounds of 155-mm HE, of Smoke Week II. The Smoke Week II trials were conducted at Eglin AFB in November 78 for PM Smoke/Obscurants.¹⁵

¹⁴ "Dust Debris Test Conducted at Ft. Sill, Oklahoma, by Dugway Proving Ground," Vols. I and II, Final Test Report by DPG, for PM for Smoke/Obscurants, Sep 79 (Unclassified).

¹⁵ "Smoke Week II: Electro-Optical (EO) Systems Performance in Characterized Obscured Environments at Eglin AFB, FL, Nov 78 (C)," DR PM-SMK 1-001-79, Mar 79, DDC No. AD0917471 (Confidential).

**PREDICTED VS. MEASURED (RELATIVE) TRANSMISSION (8-12 μ m)
EVENT B**

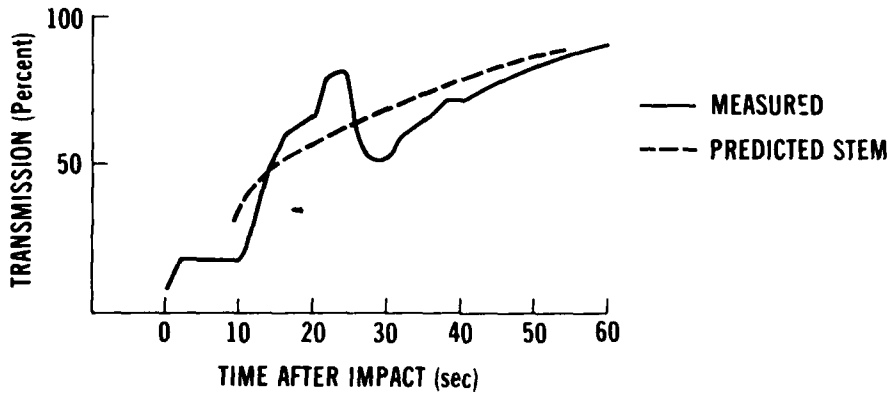


Figure 20. Predicted vs. measured transmission (8- to 12- μ m). (Graf II, 17 Nov 78) (Reference 10)

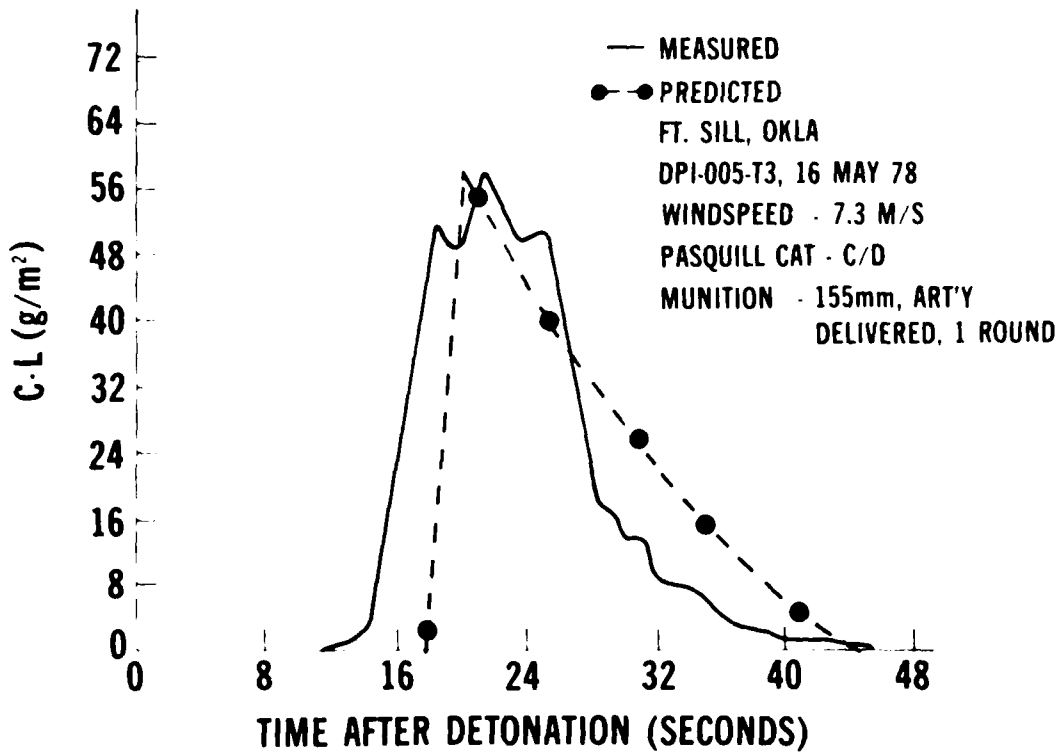
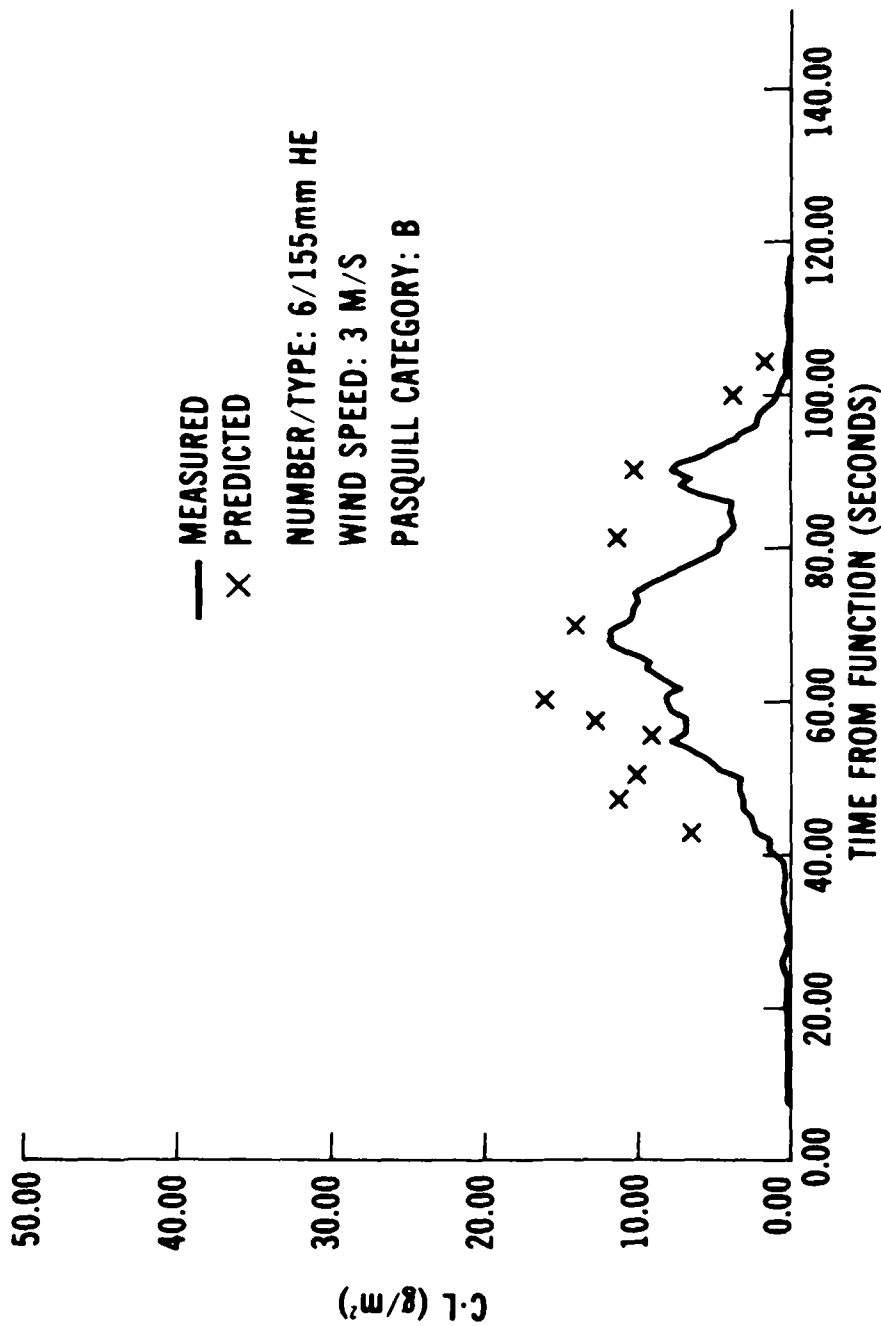


Figure 21. Comparison of HE dust model to Ft. Sill data. (Reference 14)



**CL VALUES VERSUS TIME FOR NORTH ROW
 CALCULATED USING TRANSMITTANCE AND EXTINGTION COEFFICIENT**

TRIAL #29 SWII, 16 NOV 78

Figure 22. Comparison of HE dust model to Smoke Week II data. (CL values versus time for north row calculated using transmittance and extinction coefficient.) (Trial #29 SW II, 16 Nov 78.) (Reference 15)

VII. CONCLUSIONS

The significant results from the measurements, modeling, and analyses just described can be summarized in the following manner:

1. Useful empirical models which calculate extinction due to scattering in the 3- to 5- μm and 8- to 12- μm regions through fog and snow were developed. They all scale to visibility.

2. A method to represent a system's performance sensitivity to variations in the meteorological environment was developed. This method defines the system capability, a *measure of operational effectiveness*, as the ratio of the performance range through a specified atmospheric condition to the performance range expected if there was no atmospheric degradation.

3. The meteorological conditions allowing at least a 50% recognition range capability were calculated for the TOW nightsight. This capability level is specified by a visibility of at least 1 kilometer for a large range of tank signatures in a summer and winter environment. The visibility specification is a critical meteorological parameter of the TOW system.

4. A semi-empirical model capable of predicting the effects of smoke obscuration on electro-optical systems has been developed for use in combat simulations or evaluation of smoke munitions by the Night Vision and Electro-Optics Laboratory and the General Research Corporation. The NV&EOL/GRC WP Smoke Model, a subset of the total model, has been programmed for computer use.

5. The NV&EOL/GRC WP Smoke Model is well validated to available field test data for its capability to predict cloud dimensions and transmission produced by static deployment of instantaneous WP. Aspects of the smoke model which have not yet been resolved because of a lack of data include the effects of high relative humidity on the yield factor and the effects of artillery-delivered smoke.

6. The HE Dust Model developed by GRC compares well with field data and offers a viable tool for the analysis community.

DISTRIBUTION FOR NV&LOL REPORT DELNV-TR-0016

| No. Copies | Addressee | No. Copies | Addressee |
|------------|---|------------|---|
| 20 | Commander ERADCOM ATTN: DRDEL-AP-OA M. Geisler Adelphi, MD 20783 | 1 | Project Manager M60 Tank System Warren, MI 48090 |
| 1 | Director Atmospheric Sciences Lab ATTN: DELAS-D White Sands Missile Range, NM 88002 | 1 | Project Manager MICV Warren, MI 48090 |
| 1 | Director CS&TA Laboratory ATTN: DELCS-D Fort Monmouth, NJ 07703 | 1 | Project Manager GLD/TTD Redstone Arsenal, AL 35809 |
| 1 | Director Electronic Warfare Lab ATTN: DELEW-D Fort Monmouth, NJ 07703 | 1 | Project Manager VIPER/AHAMS Redstone Arsenal, AL 35809 |
| 1 | Director Electronics Technology & Devices Lab ATTN: DELET-D Fort Monmouth, NJ 07703 | 1 | Project Manager AAH AVARADCOM St Louis, MO 63166 |
| 1 | Commander Harry Diamond Labs ATTN: DELHD-AC Adelphi, MD 20783 | 1 | Project Manager TADS/PNVS AVARADCOM St Louis, MO 63166 |
| 1 | Director Signal Warfare Lab ATTN: DELSW-D Vint Hill Station, VA 22186 | 1 | Commander ARRCOM ATTN: DRSAR-CP Rock Island, IL 61299 |
| 1 | Project Manager XM-1 Tank System Warren, MI 48090 | 1 | Project Manager RPV AVARADCOM St Louis, MO 63166 |
| | | 1 | Commander ARRADCOM ATTN: DRDAR-SEC Dover, NJ 07801 |

| No. Copies | Addressee | No. Copies | Addressee |
|------------|---|------------|---|
| 1 | Commander CORADCOM ATTN: DRDCO-PPA/CA Fort Monmouth, NJ 07703 | 1 | Commander NARADCOM ATTN: DRDNA-O Natick, MA 01760 |
| 1 | Commander CIRCOM ATTN: DRSEI-CP/CR Fort Monmouth, NJ 07703 | 1 | Commander AMMRC Watertown, MA 20172 |
| 1 | Commander MIRADCOM ATTN: DRDMI-CA 3 DRDMI-WP Fort Belvoir, VA 22060 | 1 | Commandant US Army Infantry School Ft Denning, GA 31905 |
| 1 | Commander MIRADCOM ATTN: DRDMI-DC Redstone Arsenal, AL 35809 | 1 | Director Defense Advanced Research Projects Agency Rosslyn, VA 22209 |
| 1 | Commander MIRCOM ATTN: DRSMI-EO Redstone Arsenal, AL 35809 | 1 | Commander US Naval Research Lab Washington, DC 20375 |
| 1 | Commander AVARADCOM ATTN: DRCAV-BC St Louis, MO 63166 | 1 | Commander HQ DARCOM ATTN: DRCCP-I Alexandria, VA 22333 |
| 1 | Commander TSARCOM ATTN: DRSTS-CO St Louis, MO 63166 | 1 | Commandant Defense Systems Management School Ft Belvoir, VA 22060 |
| 1 | Commander TARADCOM ATTN: DRCTA-VC Warren, MI 48090 | 1 | Commandant US Army Engineer School Ft Belvoir, VA 22060 |
| 1 | Commander TARCOM ATTN: DRSTA-NC Warren, MI 48090 | 1 | Commander USACSC Ft Belvoir, VA 22060 |

| No. Copies | Addressee | No. Copies | Addressee |
|------------|---|------------|--|
| 1 | HQDA ATTN: DACA-CA Washington, DC 20310 | 1 | Project Manager FIREFINDER ATTN: DRCPM-FF Fort Monmouth, NJ 07703 |
| 12 | Defense Documentation Ctr ATTN: DDC-TCA Cameron Station (Bldg 5) Alexandria, VA 22314 | 1 | Department of Defense Production Engineering Spt Otc (PEO) ATTN: D. Anderson Cameron Station Alexandria, VA 22314 |
| 1 | Commander US Army Training & Doctrine Com ATTN: AICD-AN Ft. Monroe, VA 23651 | 1 | Project Manager CAC ATTN: DRCPM-CAC Vint Hill Station, VA 22186 |
| 2 | Commander US Army Logistics Ctr Fort Lee, VA 23801 | 1 | Project Manager SOTAS ATTN: DRCPM-STA Fort Monmouth, NJ 07703 |
| 1 | Commander US Army Systems Analysis Agency Aberdeen Proving Ground, MD 21005 | 1 | Commandant US Army Armor School Fort Knox, KY 40121 |
| 1 | NASA Scientific & Tech Info Facility ATTN: Acquisitions Branch (S-AK-DE) P.O. Box 33 College Park, MD 20740 | 1 | Commandant US Army Treat Artillery School Fort Sill, OK 73503 |
| 1 | Study Center National Maritime Research Ctr King's Point, NY 11024 | 1 | Commandant US Army Air Defense School Fort Bliss, TX 79916 |
| 1 | Commander USAAVNC Ft. Rucker, AL 36862 | 1 | Director US Army Air Mobility RAD Ctr Ames Research Ctr Moffett Field, CA 94035 |
| 1 | Director NVA FOI ATTN: DEFENSE SMS SEMCO Ft. Belvoir, VA 22060 | 3 | Commander AFSC ACC Andrews AFB, MD 20334 |
| 1 | Project Manager REMBASS ATTN: DRCPM-RBS Fort Monmouth, NJ 07703 | | |

| No. Copies | Addressee |
|------------|---|
| 2 | Commander FSD/ACC Hanscomb AFB, MA 01730 |
| 1 | Commander US Naval Ordnance Lab/White Oak ATTN: Technical Library Silver Spring, MD 20910 |
| 1 | Commander Naval Electronics Lab Ctr ATTN: Library San Diego, CA 92152 |
| 1 | Armament Development and Test Ctr ATTN: DIOSE, Tech Library Eglin Air Force Base, FL 32542 |
| 100 | Director NV&IOI ATTN: DEIN V-VI (L. P. Obert) Fort Belvoir, VA 22060 |
| 1 | Commander Sacramento Army Depot Sacramento, CA 95813 |
| 1 | Commander New Cumberland Army Depot New Cumberland, PA 17070 |
| 1 | Commander Anniston Army Depot Anniston, AL 36201 |
| 1 | Dept of Defense Production Engineering Spt Otr (PE SO) ATTN: H. K. MacKechnie Cameron Station Alexandria, VA 22314 |

**DAT
FILM**